Available online at www.sciencedirect.com

SCIENCE DIRECT®

Tectonophysics 388 (2004) 271–297

TECTONOPHYSICS

www.elsevier.com/locate/tecto

Must magmatic intrusion in the lower crust produce reflectivity?

J.H. McBride[a,*], R.S. White[b], J.R. Smallwood[c], R.W. England[d]

[a]*Department of Geology, Brigham Young University, P.O. Box 24606, Provo, Utah 84602, USA*
[b]*Bullard Laboratories, Department of Earth Sciences, University of Cambridge, Madingley Road, Cambridge, CB3 0EZ, UK*
[c]*Amerada Hess Ltd., 33 Grosvenor Place, London, SW1 7HY, UK*
[d]*Department of Geology, University of Leicester, University Road, Leicester LE1 7RH, UK*

Received 1 July 2003; received in revised form 9 February 2004; accepted 13 June 2004

Abstract

The Færoe–Iceland Ridge (FIR) provides a laboratory in which to investigate the reflectivity and velocity structure of thick crust generated above a mantle plume in order to constrain models of underplating and the origins of lower-crustal layering in an environment dominated by young igneous processes. Over 600 km of common midpoint (cmp) data were collected along and across the FIR using a large airgun array with a 240-channel streamer. The interpretation of these data has been integrated with a velocity model of the crust and upper mantle along the FIR obtained from wide-angle seismic arrivals into ocean bottom and land seismometers. Due to the intermediate water depths and the presence of basalt near the water bottom, specialized processing steps were required for the cmp data. A wave equation-based multiple attenuation scheme was applied to the prestack data, which used a forward model of the multiple series to predict and attenuate multiple energy. Array simulations were applied in the shot and receiver domains in order to minimize spatial aliasing and reduce low apparent-velocity noise. Most of the sections over the central (oceanic) portion of the FIR show no pronounced reflectivity, although occasional Moho and/or lower-crustal reflections are observed. We believe that the poor reflectivity results largely from a lack of physical property contrasts rather than being an effect of acquisition or processing, although we also conclude that residual energy from strong multiple reflection remains in the final sections. Amplitude decay and reflection strength vary along the FIR, but there is good signal-to-noise ratio to travel times of at least 9 s (i.e., into the lower crust), implying that the reduced reflectivity beneath the main part of the FIR is not an artifact of signal penetration loss. We conclude that the addition of melt to the lower crust along the trace of the plume apparently did not produce strong physical property contrasts in the lower crust, where little reflectivity is apparent. Perhaps this was because the entire crust was hot at the time of formation. In contrast, igneous intrusion into preexisting continental crust (at the Færoe Islands end of the FIR) and into older igneous crust (at the Iceland end of the FIR) produces significant lower-crustal reflectivity. Strong lower-crustal reflectivity elsewhere beneath the northwestern European continental margins may have a similar intrusive origin.

Keywords: Oceanic crust; Seismic reflection; Mantle volcanism; Mantle plumes

* Corresponding author. Tel.: +1 801 422 5219; fax: +1 801 422 0267.
E-mail address: john_mcbride@byu.edu (J.H. McBride).

0040-1951/$ - see front matter © 2004 Elsevier B.V. All rights reserved.
doi:10.1016/j.tecto.2004.07.055

1. Introduction

The Færoe–Iceland Ridge (FIR) is an aseismic oceanic ridge between the Færoe Islands continental fragment and present-day Iceland. It marks the trace through time of the intersection of the Iceland mantle plume with the mid-Atlantic spreading center (Fig. 1; Bott and Gunnarsson, 1980; White and McKenzie, 1995; White, 1997; Smallwood et al., 1999). The thickness of the crust beneath the FIR is 25–30 km (Smallwood et al., 1999) compared to a global average oceanic crustal thickness away from mantle plumes of 6–7 km (White et al., 1992). The FIR is part of a longer ridge system stretching across the entire northern North Atlantic from the Færoe Islands to the eastern Greenland continental margin. This ridge system developed as part of the North Atlantic Tertiary igneous province, which formed during rifting associated with continental breakup over a large area of unusually hot mantle fed by a mantle plume (White, 1992). This igneous province consists mainly of basalt and extends almost 2000 km from the British Isles to western Greenland (Saunders et al., 1997).

At least two phases have been recognized in the development of the Tertiary igneous province, the first of which initiated ~62 Ma ago with magmatism affecting a broad area of eastern Greenland and the northwest European continental margins. The second began ~56 Ma ago and includes the submarine seaward-dipping reflector sequences typical of volcanic continental margins and the basaltic igneous rocks of Iceland and the FIR (e.g., White et al., 1987; White and McKenzie, 1989; Saunders et al., 1997;

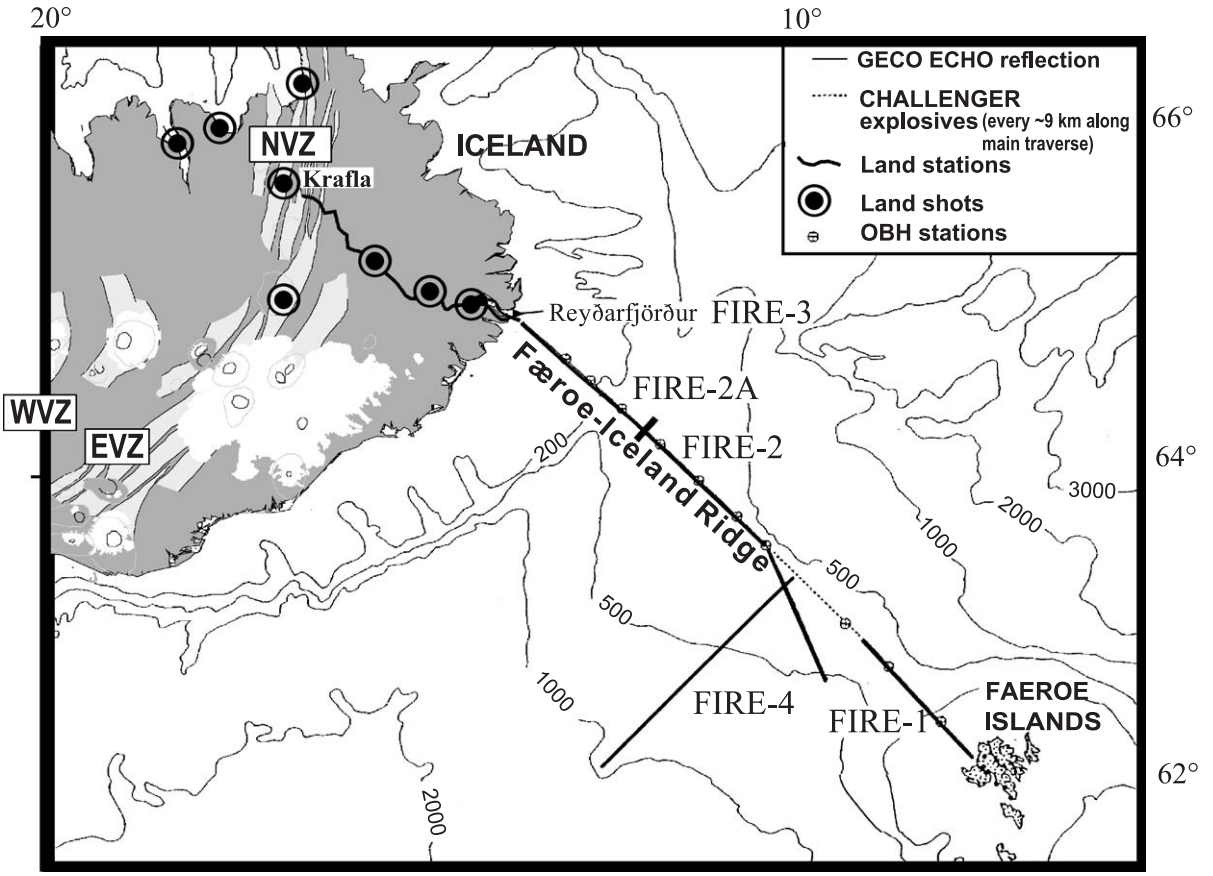

Fig. 1. Location map for FIRE cmp profiles. NVZ, EVZ, and WVZ refer to northern, eastern, and western volcanic zones of Iceland, respectively, which delineate the spreading center plate boundary between the European and North American plates.

Smallwood and White, 2002). The first phase has been attributed to the initiation of the Iceland mantle plume, while the second may be related primarily to the interaction between the mantle plume and continental breakup (Saunders et al., 1997; O'Connor et al., 2000). The mantle plume head may have had a large circular platform (White and McKenzie, 1989), or it may have been focused into tripartite or quadripartite sheets (Barton and White, 1997; Smallwood and White, 2002).

The interpretation that the FIR is oceanic crust that formed by seafloor spreading above the core of the Iceland mantle plume (Richardson et al., 1998; White et al., 1996; Smallwood et al., 1999) indicates an environment dominated by magmatic processes that added material to the crust from partial melting in the mantle. The Færoe Islands, which sit close to the eastern North Atlantic continental margin, are topped by thick (5.5–7 km) Tertiary lavas that erupted at or near the time of Tertiary continental breakup (Waagstein, 1988; Richardson et al., 1998, 1999). The crust beneath the islands may be up to 46 km thick, with significant igneous underplating or intrusion in the lower crust. The crust below Iceland was produced by interaction between the mantle plume and the mid-Atlantic spreading ridge (Darbyshire et al., 2000a,b; Maclennan et al., 2001b). It is this interaction that was responsible for the generation of anomalously thick crust along the FIR (White, 1997). At the time of formation, the FIR was probably similar to present-day Iceland, with marked subaerial topography, which is now below sea-level, due partly to thermal subsidence as the lithosphere has cooled and partly to erosion of the uppermost section.

Based on the results of the Færoe–Iceland Ridge Experiment (FIRE; White et al., 1996), the seismic P-wave velocity of the lower crust below the FIR is estimated to be 7.0–7.5 km s^{-1} (Smallwood et al., 1999; Fig. 2), which is consistent with an interpretation of intrusion of sill-like masses into the lower crust from abnormally hot mantle (mantle plume) during early Tertiary continental breakup and seafloor spreading. Enhanced lower-crustal reflectivity, as observed on deep seismic reflection records across continental crust (i.e., a "layered lower crust"; Hobbs and Peddy, 1987), has for many years been explained in terms of such magmatic intrusion, even where a candidate thermal, magmatic, or rifting event is lacking (Brown, 1987; Meissner and Sadowiak, 1992). Indeed, associating lower-crustal reflectivity with magmatic intrusion from the mantle in the presence of a rifting environment was one of the earliest outcomes of the application of the seismic method to studying the Earth's crust and upper mantle [see Allmendinger et al. (1987) for a review of early concepts]. For example, deep seismic reflection profiles from the northern North Sea (Klemperer, 1988) and the USA Basin and Range (Klemperer et

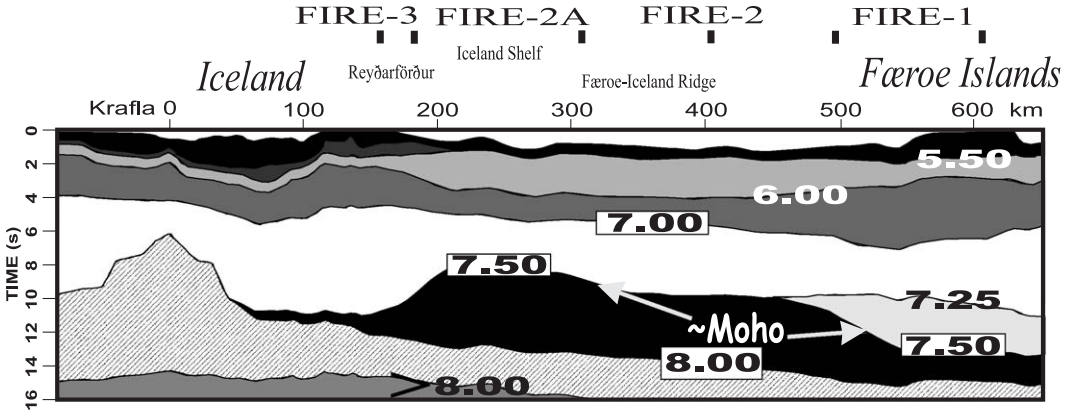

Fig. 2. Velocity model between Færoe Islands and north-central Iceland, converted from depth to travel time, showing depth interfaces defined from modeling of wide-angle arrivals based on the FIRE program with approximate velocity values (km s^{-1}; from Smallwood et al., 1999). Numbers across top indicate kilometers along the line (Fig. 8). Upper blank pattern denotes velocity less than 5.0 km s^{-1}. The Moho discontinuity is expressed as a transition in velocity from 7.3 to 7.7 km s^{-1}. We thus represent the Moho on this model as the 7.5 km s^{-1} contour.

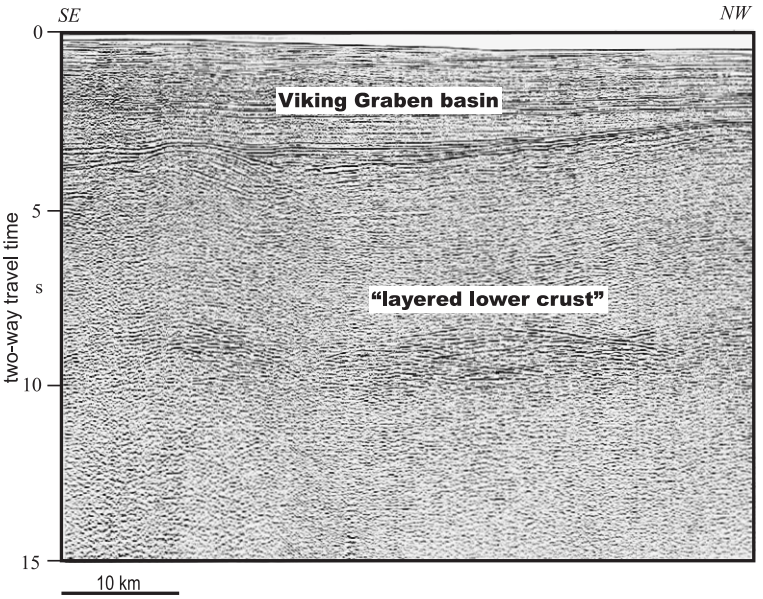

Fig. 3. Example of lower-crustal reflectivity expressed beneath the Viking Graben of the northern North Sea on excerpt of profile NSDP84-4 (from Klemperer and Hobbs, 1991). The unmigrated profile shows sedimentary reflections in the upper 4 s and lower-crustal "layering" just before 10 s. No vertical exaggeration for 6 km s^{-1}.

al., 1986) that show prominent "layering" of reflectivity in the lower crust have been explained as manifestations of their respective regional histories of continental extension and rifting (Fig. 3).

2. Purpose of study

The purpose of this paper is to present results of the FIRE common midpoint (cmp) profiles along the FIR in order to investigate the seismic reflectivity expression of a known and relatively well-constrained example of magmatic addition to the lower crust. Our particular example arises as a result of mantle plume interaction with a continental rift (Færoe Islands), with developing oceanic crust above a spreading center (main part of FIR), and with older, earlier formed oceanic-type crust (Reyðarfjörður, Iceland). The central part of the FIR furnishes one of the few cases of a lower crust and uppermost mantle that has a single-mechanism history of massive magmatic extraction from the mantle responsible for the formation of an overthickened oceanic ridge. We accordingly attempt to test the long-standing idea that such magmatic intrusion must produce the lower-crustal reflectivity commonly observed on deep seismic reflection profiles from many settings.

3. The Færoe–Iceland ridge experiment (FIRE)

3.1. Data acquisition

The Færoe–Iceland Ridge Experiment (FIRE) was a combined onshore–offshore seismic reflection and wide-angle acquisition program carried out along the FIR (Fig. 1) during the summer of 1994. Overviews of the technical design of the FIRE are given by White et al. (1996), Staples et al. (1997), Richardson et al. (1998), Smallwood et al. (1998, 1999). These previous studies have focused primarily on the wide-angle seismic refraction and diving wave portions of the recorded wave field.

The 2-D cmp seismic surveys were recorded by the M/V *Geco Echo* operated under contract to Schlumberger Geco-Prakla (now Western Geco), beginning just offshore of the western Færoe Islands and ending in the narrow fjord of Reyðarfjörður in eastern Iceland with a total of 601 km of profile acquired (Fig. 1). The survey parameters were designed so as

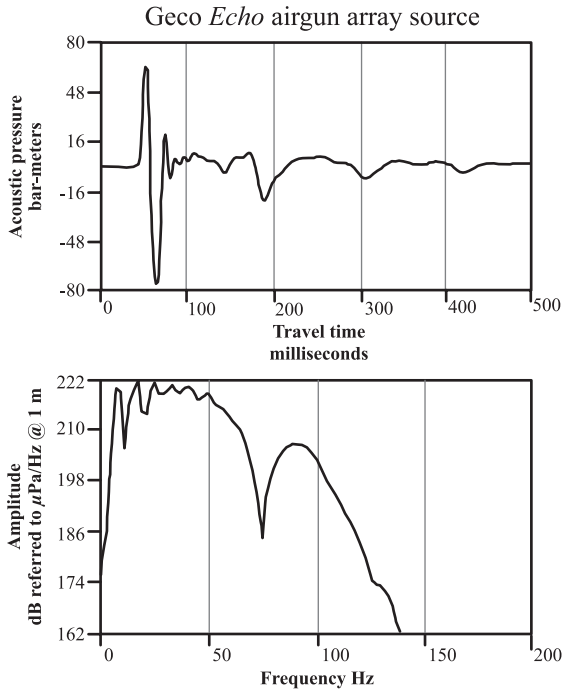

Fig. 4. Airgun array source signature (top) and amplitude spectrum (bottom) used for the FIRE cmp program. The airgun source array and depth were designed to enhance low frequencies while preserving a broad bandwidth.

to maximize the penetration of low-to-moderate frequency signal through the expected thick volcanic pile along the FIR and into the lower crust and upper mantle. A large tuned airgun array (Fig. 4) was employed with a total volume of 153 l (9324 in.^{3}) divided into six subarrays pressurized at 140 bar (2000 psi). The size of the 36 airguns ranged from 30 to 500 in.^{3}. Each subarray included one bolted cluster of airguns near the vessel's stern, consisting of either 585 or 465 in.^{3}, in order to provide increased accuracy and stability.

Modeling of different combinations of airgun array and hydrophone towing depths led us to choose depths of 10 ± 1 m for the airguns and 18 ± 1.5 m for the hydrophone streamer, in order to produce a seismic source possessing a combination of low- and moderate-frequency components (Fig. 4). The deeper than usual streamer depth resulted in a desirable shift in energy into lower frequencies. The bubble source had a peak-to-peak amplitude of 144 bar m (Fig. 4), which is relatively large for petroleum industry surveys. The recording system was a NESSIE III with 240 channels (25-m group interval; 48 hydrophones per group), which recorded airgun shots at 4-ms sample rate every 75 m along a 6000-m-long hydrophone streamer (except 3000 m in Reyðarfjörður). Total recording time was 27 s.

Weather conditions were excellent during the entire survey with wind not exceeding Force 5 and seas not higher than 2 m. The sole logistical problem was a barrage of fishing drift nets deployed across the track of the FIR northwest of the Færoe Islands, which required the deviation shown in the survey in Fig. 1 (White et al., 1996).

3.2. Data processing

3.2.1. Overview

We anticipated that acquisition and processing of seismic data from the FIR would present significant challenges. Accordingly, processing was aimed toward reducing the effect of strong multiple reflections generated within the upper crustal layered basalts, toward the elimination of low apparent-velocity noise due to shallow scattering, and toward the enhancement of weak primary reflections from the lower crust and upper mantle (Table 1). The data were processed by Western Geophysical under supervision by the British Institutions Reflection Profiling Syndicate (BIRPS). The strategy used in designing the processing parameters consisted of choosing six test panels of data from the five profiles, each of which were divided into three

Table 1
Data processing summary

Resample to 8 ms
Low cut frequency filter (6 Hz 12 dB/octave)
Wave equation multiple attenuation
Shot and receiver domains array simulation
Velocity analysis
Spherical divergence compensation (based on stacking velocities)
Predictive deconvolution
Low cut frequency filter (4 Hz 8 dB/octave)
CMP Sort
NMO, forward mute & stack (40 nominal fold of cover)
Frequency–wave number filter (pass signal −6 to +6 ms/trace)
Adjacent trace summation (to 25-m cmp interval)
Predictive deconvolution
Time-variant band-pass frequency filter
Time-variant instantaneous automatic gain control

travel time segments: from the seabed to 4 s below it ("upper crust"); the next 4-s interval ("middle-to-lower crust"); and the next 4-s interval below that ("lower crust to uppermost mantle"). These panels were used as standards throughout the processing. We next describe those aspects of this processing stream that were

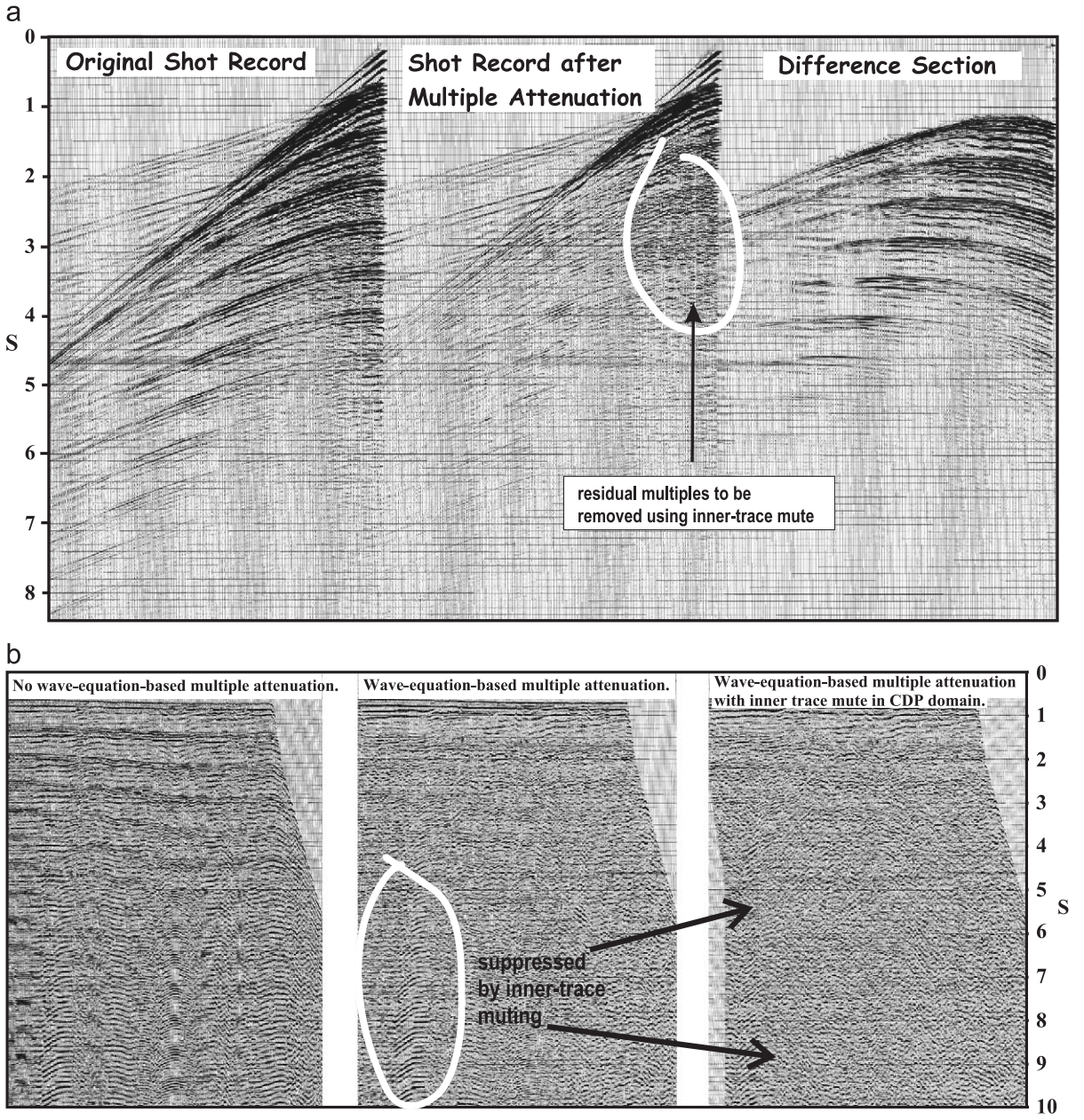

Fig. 5. (a) Example of shot record from FIRE-2 before and after application of wave equation-based multiple attenuation, based on water velocity (10°–50° dip limits) showing how strong water-bottom multiples generated by high-velocity basalts are attacked by this processing step. Also, indicated is strong residual multiple energy to be later removed. The difference section has an antialias linear move-out applied. (b) As above but displayed as stacked data. Processing includes array simulations in shot and receiver domains, band-pass filtering (6 Hz/12 dB-40 Hz/48 dB), and 1-s window automatic gain control.

especially important for enhancing weak signal in the presence of noise.

3.2.2. Multiple reflections and multiple attenuation

The most challenging aspect of the data processing was attenuating multiple reflections generated by shallow layered basalts. The portion of the FIR beneath our cmp profiles is an environment where strong multiple reflection has definitely occurred. Seafloor depths along the profiles mostly ranged between 100 and 500 m. Using refracted first arrivals recorded by the *Echo* from the airgun shots, Smallwood et al. (1999) derived a shallow (maximum depth ~2 km below sea level) P-wave velocity model that delineates several small sedimentary basins up to 400 m thick along the crest of the ridge. These small basins, which could produce "pegleg" multiples on the sections below, were interpreted as caused by a combination of tectonic movements along the ridge and the action of currents (Smallwood et al., 1999). The shallow refractions also indicate seabed P-wave velocities of 4.0–4.5 km s^{-1} on the ridge and greater than 4.5 km s^{-1} on the Iceland and Færoe shelves, which are attributed to subcropping basalt flows. Areas, such as ours, where the velocity of the shallow upper crust is high with respect to the water (i.e., basalt is at or near the seabed), produce a "hard" water bottom, which is conducive to the generation of multiples. The danger is that most of the seismic source energy is trapped in the water column with little remaining that penetrates into the rocks below, resulting in weak primary overlain by strong multiple reflections (Matson et al., 1999).

We employed a four-step sequential approach to assess multiple attenuation procedures: (1) wave equation multiple suppression; (2) a demultiple filter applied in the frequency–wave number (f–k) domain; (3) inner trace muting on shot records; and (4) standard predictive deconvolution applied before and after stacking. In addition to a routine series of steps used in seismic data processing, a wave equation-based multiple attenuation scheme was applied to the pre-stack data. This procedure involved the production of a forward model of the multiple series based on the original multiple-contaminated data that was used to predict the "free-surface" multiple response of the air–water interface (Matson et al., 1999). The predicted multiple wave field is then subtracted from the original data (Wiggins, 1988; Fig. 5a, b). The success of the process, which is applied early in the processing in the shot domain (Table 1), depends on the correct selection of parameters used to define the multiple model. These include (1) the water velocity (1475 m s^{-1}), (2) an

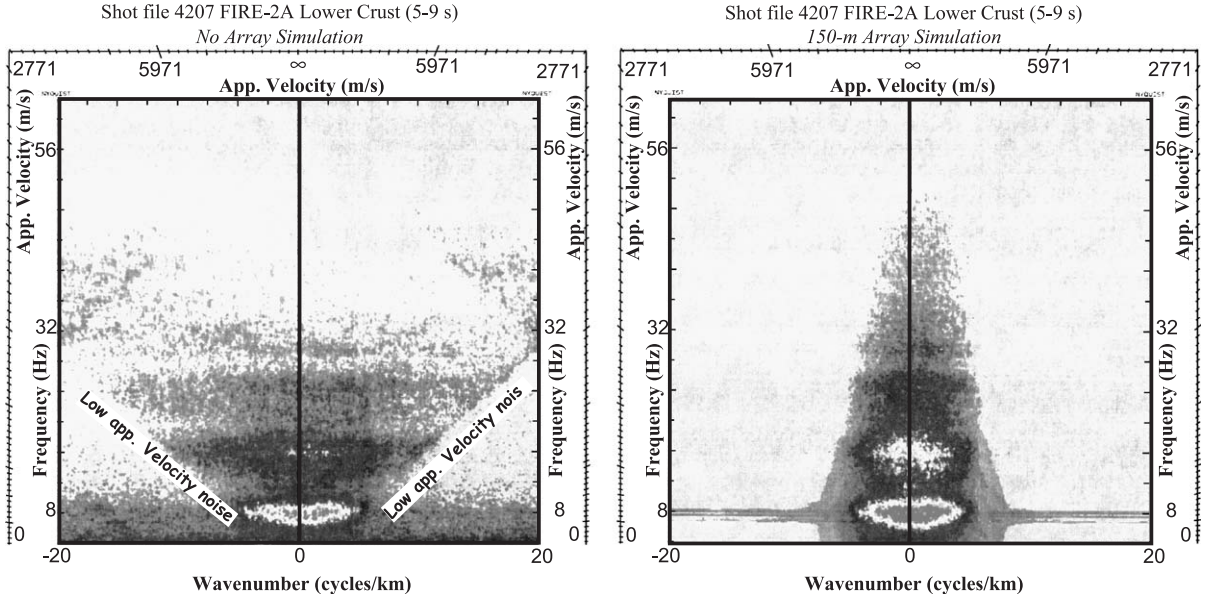

Fig. 6. Frequency–wave number spectra for unprocessed lower-crustal reflectivity showing strong contamination by low apparent-velocity noise (left) and the result of weighted array simulation applied in the shot domain (right).

antialias shift (8 ms/trace) in order to avoid spatial aliasing, (3) a water-bottom shaping operator (150-ms length) used to compensate for errors in picking the water-bottom arrival, including frequency-dependent effects, (4) the lead time (50 ms) used in order for the operator to represent both advances or delays in arrival time, (5) the number of design windows (20) that are required to represent each repeated multiple, and (6) dip filters (+50° to −10°) used to avoid spatial aliasing in the *f–k* domain.

An *f–k* demultiple filter was tested using a decreasing percentage (90% at 0 s to 50% at the bottom of the record) of the derived stacking velocities. This approach seeks to attenuate, based on apparent-velocity, multiple reflections in the cmp domain that will show a greater amount of uncorrected normal move-out compared to higher-velocity primary reflections arriving at the same time. The testing indicated that this process did little to improve the final stacks and was therefore not used (Table 1); however, it was used as part of the velocity analysis in order to clarify the primary velocity function. An inner trace mute was tested on FIRE-1, which was deemed successful at removing multiple energy associated with multiple diffractions (Fig. 5b). Deconvolution was applied before stacking with two design windows (near offset ranges: water bottom + 200 to 6000 ms; 6000 to 11000 ms) with gap and operator lengths of 32/392 ms and 48/528 ms, respectively. Poststack deconvolution was applied with larger gaps (48 and 64 ms, respectively) for the same design windows (Table 1).

3.2.3. Array simulation and apparent-velocity filtering

An array simulation was tested and applied in the shot and receiver domains in order to minimize spatial aliasing and attenuate low apparent-velocity noise (Fig. 6). Low apparent-velocity noise arising from shallow scatterers is a common problem for marine deep

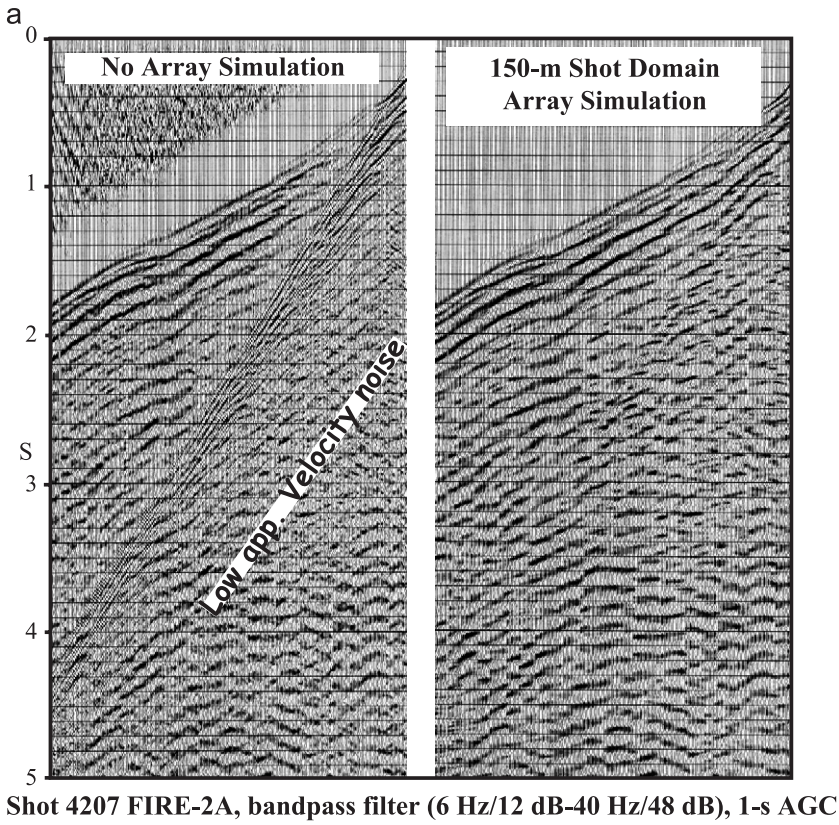

Fig. 7. (a) Example of low apparent-velocity noise contamination due to scattering generated by high-velocity basalts on a shot record and the result of array simulation. (b) Same as above in the stack domain.

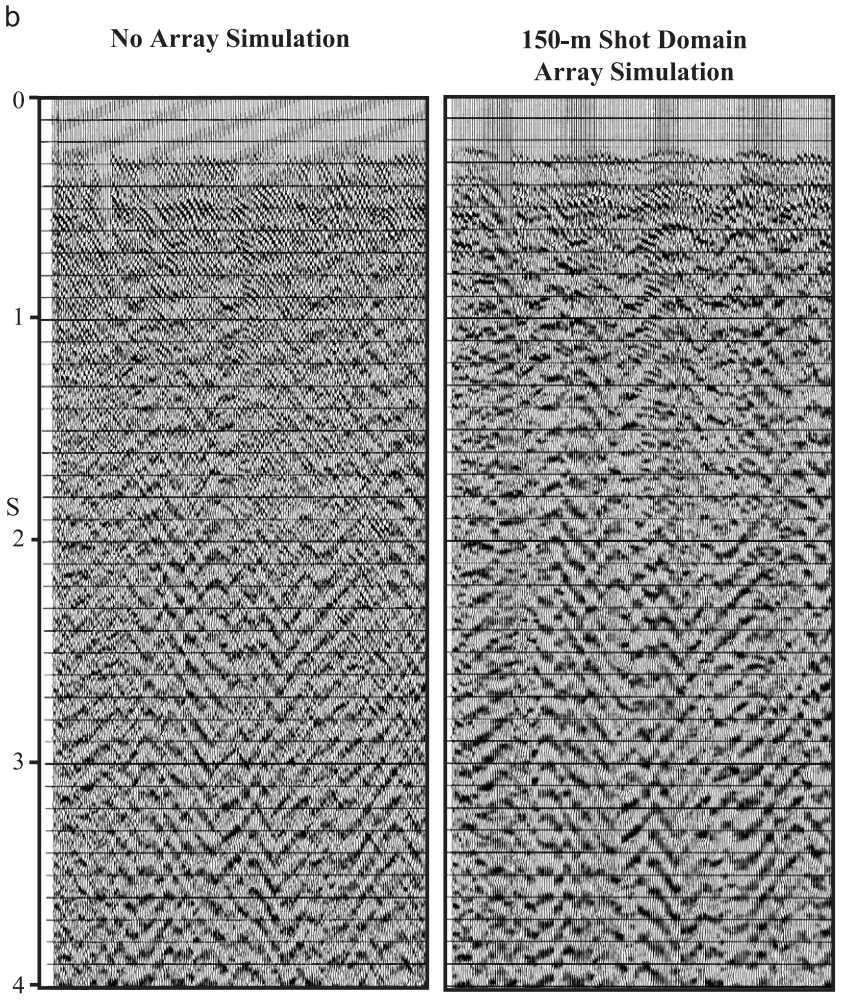

Fig. 7 (*continued*).

seismic reflection data (Klemperer, 1988) and can severely mask primary reflections and interfere with subsequent data processing steps. Four simulated receiver arrays were tested in the shot domain. For example, a "50-m" receiver group interval was simulated by weighting five adjacent traces as 0.1, 0.5, 1.0, 0.5, 0.1. Similar simulations were tested for 100-, 150-, and 200-m group intervals. Three source arrays were simulated in the receiver domain. For example, a "50-m" source array was simulated by weighting three adjacent traces as 0.1, 1.0, 0.1. Sources of "100-m" and "200-m" arrays were also tested. The best simulation used a "150-m", 11-trace array in the shot domain followed by a "100-m", 5-trace array in the receiver domain (Fig. 7a). The order of applying the wave equation demultiple and the array simulations was tested. It was decided that applying the wave equation demultiple before the combined array simulations produced the best result (Fig. 7b).

F–k filtering was tested poststack in order to remove low apparent-velocity events associated with scattering. Tests were performed for dips of ±3, 6, 9, and 12 ms/trace for the three travel time windows. A filter passing dips between +6 and −6 ms/trace was

found to be optimum followed by adjacent cmp trace summation from 12.5 to 25 m (Fig. 6).

3.2.4. Band-pass frequency filtering

Various combinations of time-variant band-pass frequency filters were tried, from 7.5 to 60 Hz. This range of options corresponds to the range based on the modeled source signature (Fig. 4) from the lower frequency to the position of the first notch in the spectrum caused by the streamer depth. The optimum low-cut to high-cut filter combination was (in Hz/dB per octave) 7.5/15–60/48 for 0 to 4 s; 7.5/15–40/48 for 4 to 10 s; and 7.5/15–30/48 for 10 to 17 s.

3.2.5. Instantaneous time-variant automatic gain control

Various window lengths for applying instantaneous automatic gain control were tested in order to produce the optimum balance between primary reflections and background noise as it changed within the crust and mantle. Five different window lengths were tested from 250 to 4000 ms. The optimum time and window combination was chosen (in ms) as (0, 250), (2000, 250), (3500, 500), (4500, 1000), (6000, 2000), and (17000, 4000).

3.2.6. Further poststack processing

Final displays of the sections were made using Landmark Graphics' ProMAX2D™. The final steps included the application of a low apparent-velocity rejection filter using a limited aperture tau-p (zero offset travel time intercept–slowness) transform (e.g., Yilmaz, 1987), and in order to display the final cmp stacked sections at small scale and further reduce noise, we blended (1:1) the output data with the absolute value of the amplitude squared and displayed as variable area with no wiggle trace and with an adjacent trace mix. Because we are primarily interested in the general pattern of reflectivity, the sections are displayed with a phase-shift migration at water velocity only.

4. Results

4.1. Overview

During the data processing stage, we believe we were successful in removing the majority of the multiple reflected energy from the stacked cmp sections. The success of multiple rejection techniques aids in revealing the genuine primary reflectivity character of the crust and upper mantle beneath and across the FIR (Fig. 6). Most of the sections over the oceanic portion of the shelves and especially the ridge show little pronounced reflectivity when compared with sections from the North Sea (see Klemperer and Hobbs, 1991 for a review). We consider this relative lack of reflectivity to be mostly indicative of the lack of physical property contrasts rather than an effect of acquisition or processing. Significant incoherent deep-water residual multiple energy undoubtedly remains; however, we believe that strong reflection layering, like that observed beneath Reyðarfjörður (FIRE-3; see discussion below), if present would be detectable at least somewhere on the FIR sections (northwestern part of FIRE-1, FIRE-2, FIRE-2A). Likewise, prominent layering is not observed on FIRE-4 (not shown herein).

The most prominent events on the FIR profiles are occasional reflection groups arriving at Moho travel times, clusters of locally more significant horizontal reflectivity, and rare sequences of dipping or subhorizontal reflections (Fig. 8). In general, the reflectivity of the FIR crust can be characterized by short reflection segments. As pointed out by Levander et al. (1994), for a typical crustal velocity of 6.3 km s^{-1}, frequencies of 10–40 Hz, and a target depth of 20 km, the Fresnel zones are about 4.5–1.4 km across. This means that many of the observed reflection segments could be below the expected Fresnel zone diameter and thus may be spurious. This would be especially true for short reflections deeper than 10 s, where the maximum frequency is filtered to 30 Hz. Accordingly, we have produced interpretive line drawings of the records for the entire cmp profiles along the FIR, in which longer coherent reflections have been noted (Fig. 8). While this procedure is obviously subjective to a degree, it provides a means to distill from the data the main reflectivity patterns. The presentation of line drawings is supplemented by excerpts of actual data records (Fig. 9).

The velocity model of Smallwood et al. (1999) (Fig. 2), based on the FIRE wide-angle seismic records from ocean bottom seismometers, was

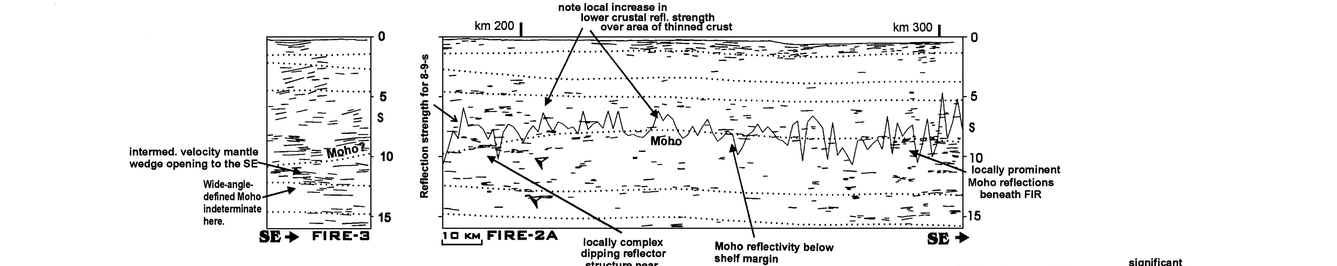

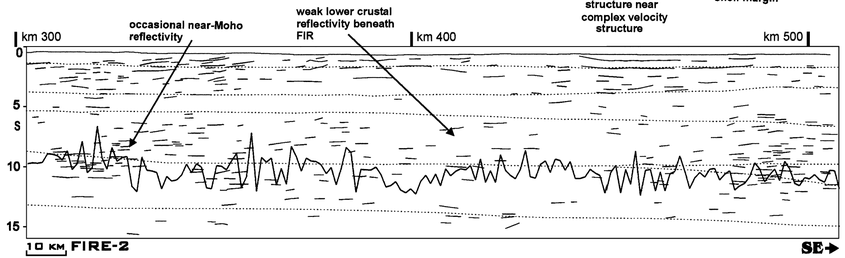

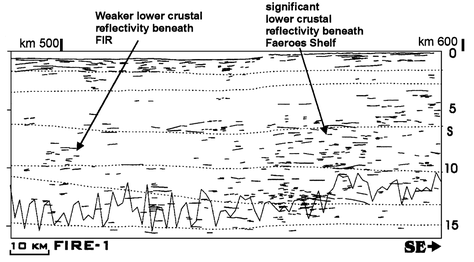

Fig. 8. Summary line-drawing interpretation of cmp FIRE profiles. See text for more information on how drawings were constructed. Boundaries from the velocity model of Smallwood et al. (1999) are superimposed (see Fig. 2 for identifications). For profiles 1, 2, and 2A, reflection strength curves (vertical scale is arbitrary; for comparison only) are also shown for the 8- to 9-s interval (see text for more explanation).

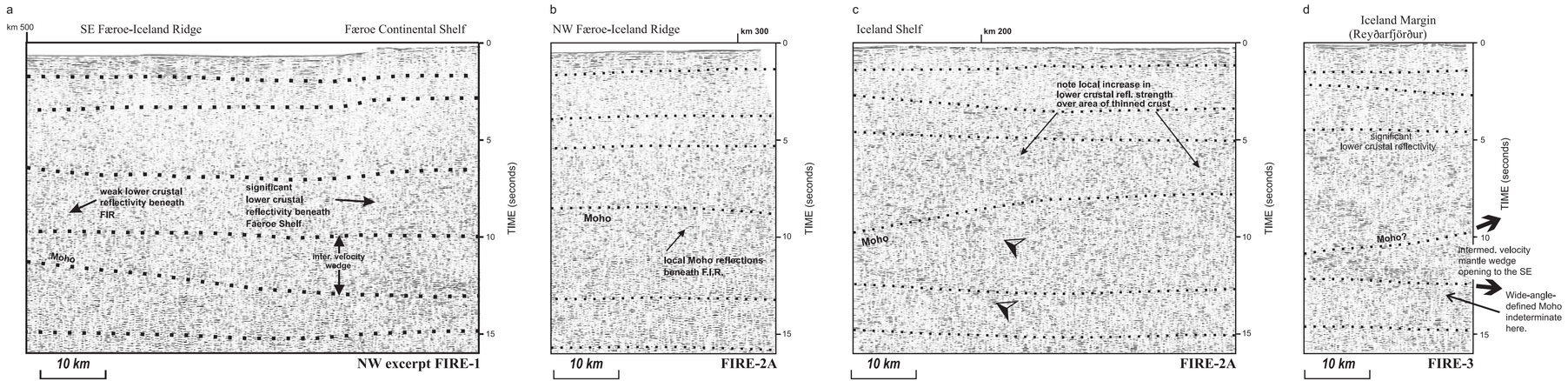

Fig. 9. Excerpts of FIRE cmp stacks, phase-shift migrated at 1500 m s^{-1} with a trace mix and tau-p transform-based coherency filter (see Table 1). (a) Central part of FIRE-1. (b) Southeastern part of FIRE-2A over approximate center of the FIR. (c) Northwestern part of FIRE-2A over the Iceland margin. Arrows indicate locally complex dipping reflector structure near complex velocity structure. (d) All of FIRE-3.

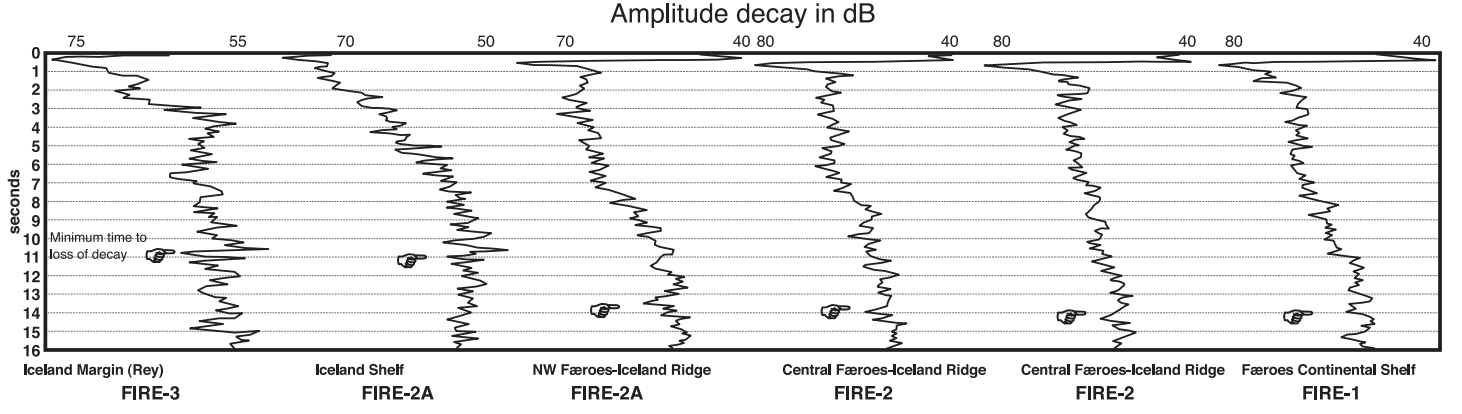

Fig. 10. Amplitude decay computed from two adjacent summed NMO-corrected cmp gathers with multiple removal techniques applied and after correction for geometrical spreading (using interval velocities). Minimum time to loss of decay is shown. The result shows persistent decay (and thus signal preservation) at least into the lower crust, implying that poor reflectivity is not an artifact of signal loss. The six panels correspond approximately to the six locations shown by triangles in Fig. 11.

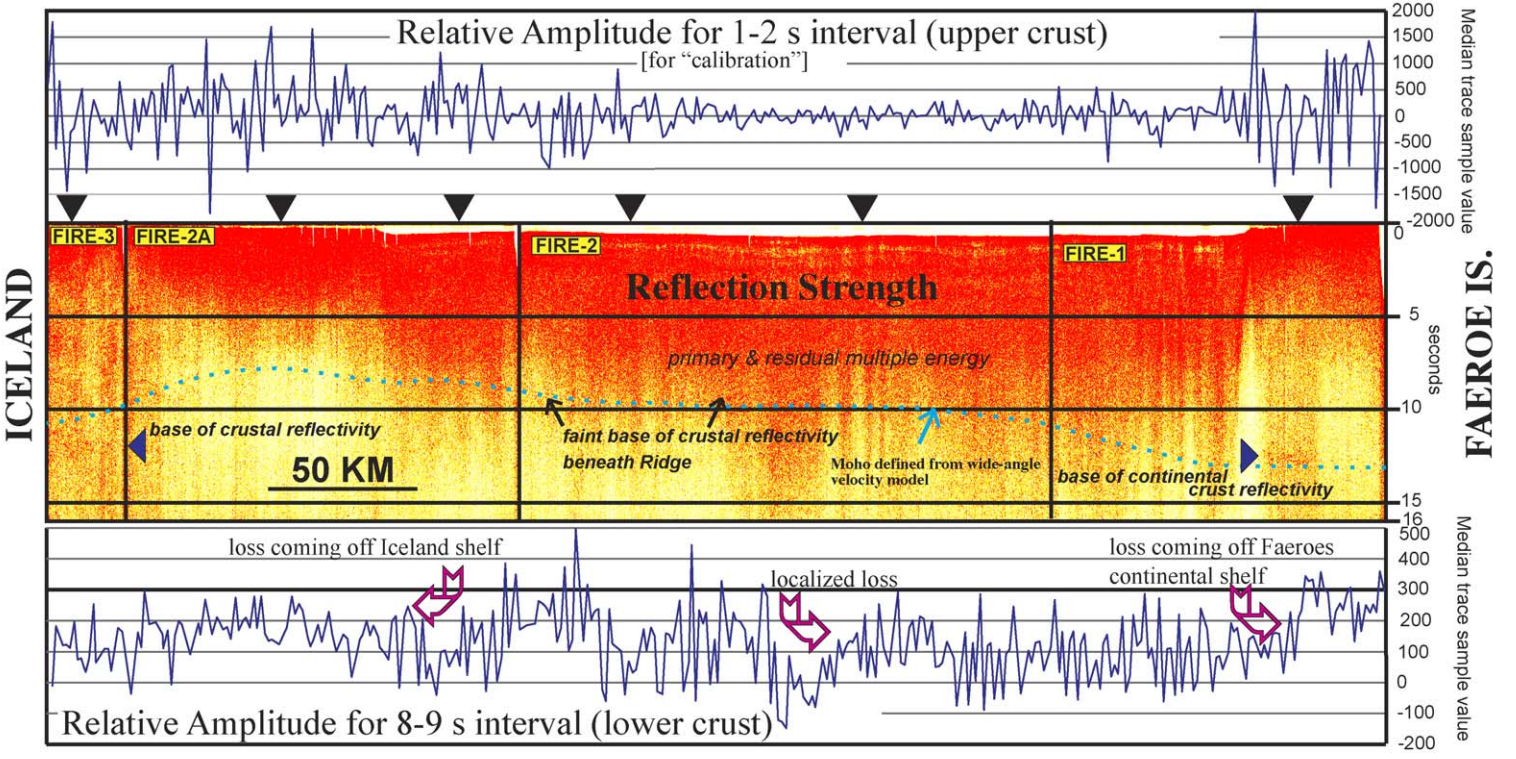

Fig. 11. Generalized reflection strength plotted as red-to-yellow variation (see text for more information). Strength varies laterally along the transect, showing slight losses into the deeper water of the Faeroe–Iceland Ridge; however, the lack of major lateral changes in reflection strength suggests that signal penetration does not vary drastically along the transect, and that the poor reflectivity beneath the Ridge is due to an actual lack of physical properties contrast in the lower crust. The six triangles indicate approximate locations of the six panels shown in Fig. 10. This analysis implies persistent signal penetration along transect.

converted to two-way travel time and was superimposed over the cmp records. We also produced amplitude decay curves in order to assess the effectiveness and variation of signal penetration along the FIRE lines (Fig. 10). Amplitude decay was computed from two adjacent summed NMO-corrected cmp gathers with multiple removal techniques applied and after correction for geometrical spreading (using interval velocities derived from velocity analyses). Finally, we derived curves showing the lateral variation in reflection strength (Hilbert transform) for the 8- to 9-s travel time interval, which corresponds approximately to the transition between the lower crust and the upper mantle and for the full sections (Fig. 11).

We display the cmp sections to 16 s because this is approximately the limit of the velocity model (Fig. 2), and because little or no interpretable reflectivity is observed later on the profiles. The FIRE-4 profile is not discussed here because results pertaining to our study are essentially the same as for FIRE-2.

4.2. Shelf–ridge transitions

The Færoe continental shelf (eastern part of FIRE-1; Fig. 8) produced some of the most prominent reflectivity from the survey with relatively clear arrivals corresponding approximately with the Moho discontinuity as determined from modeling of FIRE wide-angle and refracted arrivals (Richardson et al., 1998; Smallwood et al., 1999). The strongest of these occurs just at the break in slope of the Færoe continental margin (Figs. 8 and 9a). In general, the crust beneath the shelf is more reflective than that beneath the adjacent ridge. The lowermost crust, corresponding to the intermediate velocity wedge beneath the Færoe shelf (presumed to comprise intruded sills), is especially reflective compared to the lowermost crust elsewhere on the FIR (Fig. 9a). Along FIRE-1, both the shelf and the ridge show layered reflection sequences in the upper 2.5 s, although some of this may be residual multiple energy. In general, the upper mantle section beneath the Moho displays sparser and less-coherent reflectivity than the overlying crustal section (Fig 8).

The Iceland shelf–ridge transition off eastern Iceland (FIRE-2A) reveals a similar pattern of subhorizontal reflectivity arriving at Moho travel times with a somewhat more reflective crust compared to the adjacent ridge (Figs. 8 and 9b, c). Northwest of 200 km, reflectivity between 5 and 12 s is higher in density than beneath the ridge (Fig. 8). Beneath the northwestern part of the eastern Iceland shelf, complex dipping and/or subhorizontal reflector structure appears at and after Moho travel times (Figs. 8 and 9c). A local increase in reflectivity and reflection strength occurs in the lower crust over the area of thinner crust beneath the shelf (Figs. 8 and 9c). At the southeastern end of FIRE-2A near the center of the FIR, reflections appear at 8–9 s (Moho?) and continue into the upper mantle (Fig. 8). As on the Færoe shelf and adjacent ridge, reflectivity from the middle crust is relatively muted. Large volumes of crust are almost devoid of credible reflections.

4.3. Along the Færoe–Iceland ridge

The FIRE-2 profile was surveyed entirely along the FIR over water depths only slightly greater than that of the adjoining margins (Fig. 8). We might have expected a minor increase in multiple contamination over the ridge due to the increased water depth (i.e., fewer but relatively stronger multiples); however, no major differences were observed except possibly in the upper 1 s below the seabed, where occasional residual multiple energy remains. The upper 5 s of FIRE-2 (Fig. 8) shows broad sequences of flat and gently dipping reflections as observed by Smallwood et al. (1999). The overall deeper reflectivity pattern is similar to that of the ridge portions of FIRE-1 and FIRE-2A, adjacent to the two shelf areas on either side. The overall reflectivity is weak except in the upper 2 s. Occasional reflections appear near the Moho and in the lower crust, and track the eastward deepening of the crust–mantle boundary as determined independently from the velocity model (Fig. 2; e.g., northwestern part of FIRE-2, ~km 325; Fig. 8). Except for the Moho discontinuity, the reflection character does not change drastically between the lower crust and mantle along the FIRE-2 profile. Indeed, an important observation for the FIR is that there is no significant difference in reflectivity of the lower crust versus the uppermost mantle.

4.4. Reyðarfjörður fjord in eastern Iceland

Just before the conclusion of the cmp reflection survey along the FIR, we reconfigured the hydrophone streamer from 6000 m (240 channels) to 3000 m (120 channels) in order to navigate safely the narrow fjord of Reyðarfjörður in eastern Iceland, where we recorded a short profile (FIRE-3; Fig. 1). Results of the wide-angle seismic modeling for shots at sea recorded into three-component seismometer arrays deployed on land in Iceland are given in Staples et al. (1997). Smallwood et al. (1998) presented a synthetic seismogram modeling study of the reflectivity on FIRE-3 in order to quantitatively compare the lithology of the thick lava pile observed on the sides of Reyðarfjörður and in a 2-km-deep borehole at the head of the fjord, with dipping reflections in the upper 5 s of the profile.

The presentation of FIRE-3 herein (Figs. 8 and 9d) incorporates the final processing described above. The expected near-seabed geologic environment for FIRE-3 is similar to that for the other parts of the FIRE program in that basalt flows with velocities of up to 5.25 km s^{-1} subcrop below the profile (Smallwood et al., 1998). FIRE-3 shows relatively prominent and coherent reflectivity throughout the 16-s record (Fig. 9d), in marked contrast to the profiles along the main central part of the FIR. The upper 5 s is marked by subhorizontal and moderately northwest-dipping reflections. The dipping reflections were interpreted by Smallwood et al. (1998) as the subsurface manifestation of the subaerially erupted lavas observed in outcrop in the fjord and were considered to be similar in seismic expression to seaward-dipping reflections typical of volcanic continental margins. Lower-crustal reflectivity is more prominent and consists of bright horizontal reflections (e.g., arriving at 6 s below northwest end of FIRE-3) and later complex northwest- and southeast-dipping reflections just above the possible Moho level, which may correspond to the top of an intermediate velocity wedge of material that opens up to the southeast (Fig. 9d; Smallwood et al., 1999). This deeper wedge, which is also highly and complexly reflective, is marked by a prominent and continuous reflection boundary at 12–13 s (Fig. 9d). Somewhat weaker subhorizontal reflections persist beyond the base of the wedge into the upper mantle down to the bottom of the 16-s record. The part of northeastern Iceland, across which Reyðarfjörður traverses, consists of older Icelandic crust, which is now being reintruded by younger basalts as a result of ridge jumps (Smallwood et al., 1999).

4.5. Overall reflectivity variation and amplitude decay

In order to assess the generalized reflectivity character of the entire FIRE cmp program (FIRE-4 excepted), we computed reflection strength (Hilbert transform) using the intermediate stacks of the records with no automatic gain control or spherical divergence amplitude recovery applied (i.e., "true amplitude"; Fig. 11). We also computed relative amplitude variations laterally along the transect for two travel time intervals (1–2 s, "upper crust"; 8–9 s, "lower crust"; Fig. 11). For the upper crust, it is clear that the reflection amplitude varies much more on the shelves than over the ridge but without any noticeable overall shifts. On the other hand, for the lower crust, the variability is less but does reveal slight losses into the deeper water of the FIR coming off the shelves; however, the lack of major lateral changes in reflection strength suggests that signal penetration does not vary drastically along the transect, and that the poor reflectivity beneath the FIR is due to a genuine lack of physical property contrasts in the lower crust.

The display of generalized reflection strength (Fig. 11) varies laterally along the transect and is generally tracked in travel time by the Moho discontinuity, except for beneath the western Færoe continental margin. For example, the base of stronger reflectivity beneath the FIR corresponds to the deeper Moho there compared to the shallower reflectivity base corresponding to the shallower Moho beneath the Iceland shelf (Fig. 11). Amplitude decay curves (Fig. 10) show persistent decay (and thus signal preservation) at least into the lower crust, suggesting that poor reflectivity is not an artifact of signal loss. We are aware that amplitude decay may be a poor indicator of signal penetration in regions where high scattering occurs, which would "transfer" energy from the coherent wave field to the incoherent wave field. Thus, because multiple reflection suppression techniques attack only the coherent part of the signal, residual energy may remain especially

in the upper part of the sections where they would be strongest. Nevertheless, the amplitude decay (Fig. 10) and reflection strength (Fig. 11) plots do not show clear periodic behavior in the lower crust as would be expected from significant residual multiple contamination.

5. Discussion and conclusions

A principal impetus for the FIRE program was to investigate the seismic reflectivity and velocity structure of thick igneous crust generated in the setting of the Iceland mantle plume. The results can be used to constrain models of underplating and the origins of lower-crustal layering in a 'simple' geological environment dominated by young igneous processes. A leading paradigm that has guided much of the interpretation of deep seismic reflection data is that a "layered lower crust", which has been observed in a variety of geologic provinces worldwide (e.g., Fig. 3), is produced either by magmatic underplating sourced by mantle melting or by shear zones produced during deformation. For example, Warner (1990) considers the three possible explanations for lower-crustal layering of free aqueous fluids, shear fabrics, and basaltic underplating. He invokes the association between areas of strong horizontal lower-crustal reflectivity and known continental extension, principally the Mesozoic and Cenozoic North Sea rift basins, in order to support the third possibility. This inference has been widely applied to deep seismic reflection data sets in many settings (e.g., Allmendinger et al., 1987; Brown, 1987; Meissner and Sadowiak, 1992; Meissner and Tanner, 1993).

However, it should be obvious that an environment of major continental rifting and extension, exemplified by the USA Basin and Range and the North Sea (Klemperer et al., 1986; Klemperer, 1988; Klemperer and White, 1989), could also be expected to produce strong deformation fabrics in a mechanically weak lower crust expressed as a "layered lower crust" (e.g., Reston, 1990). For a geologic province with a polyphase history (i.e., most geologic provinces), it could also be argued that lower-crustal reflectivity need not be uniquely associated with the latest tectonomagmatic event but could simply be inherited from a previous, unrelated event (Watts et al., 1990; Prussen, 1991; McBride and England, 1999). As pointed out by Singh et al. (1998), it is not easy to associate a magmatic underplating event with a layered reflection sequence in the lower crust unless the age of the sequence is known.

In short, we have been unable to offer a unique interpretation for the observation of lower-crustal reflectivity, and moreover have been unable to say that magmatic underplating must always produce such reflectivity. Answering the latter question would reduce the ambiguity in addressing the former. The results from the FIRE cmp program now allow us to do this, because the age and origin of the lower crust (and thus its reflectivity) beneath the FIR are known.

We interpret the results of the FIRE program to indicate that the reflectivity of the lower crust and uppermost mantle beneath the FIR is poorly developed. As discussed in preceding sections, the possibility of residual multiples over the FIR obscuring any primary reflection, in combination with possibly increased heterogeneity (and thus increased scattering) in the ridge basalts (Hobbs, 2003), requires us to be cautious with our interpretation of the cmp data over the ridge. We believe that strong reflection layering, like that observed beneath Reyðarfjörður or beneath other areas of strong primary reflection layering (e.g., Fig. 3), if present would be detectable somewhere on the FIR sections; however, the ridge sections are mostly poorly reflective. Given the single-phase history of the lower crust of the FIR, we conclude that the addition of melted mantle derivatives to the lower crust, as would be expected by the effect of the Iceland mantle plume between the Færoe Islands and Iceland, did not produce significant physical properties contrasts in the lower crust. This would mean that processes of lower-crustal addition thought to have operated along the ridge need not be considered as a general cause of well-developed lower-crustal reflectivity elsewhere. Obviously, such a conclusion has the philosophical disadvantage of seeming to be an "absence of evidence equaling an evidence of absence" argument. However, we believe that the poor showing of reflectivity is not an artifact of no signal penetration nor of failure to image what would be expected to be a simple horizontal reflector series. The parameters used in the acquisition and processing, described in the foregoing sections, were designed specifically to maximize the chances of

signal penetration: (1) use of a large energy source which was biased toward low frequencies that would be most likely to penetrate the crust; (2) use of a long hydrophone streamer in order to maximize NMO-based multiple discrimination and cancellation; (3) extensive testing and successive application of a suite of multiple attenuation processes applied in different domains; (4) application of processing to reduce noise and enhance weak horizontal reflections. The analysis of the lateral and vertical amplitude variations along the profiles indicates continued signal penetration into the lower crust irrespective of location (e.g., whether on the margins or on the ridge; Figs. 10 and 11).

Lastly, despite the overall poor reflectivity of the lower crust, several areas along the FIRE profiles discussed herein show distinct reflections from the lower crust and upper mantle (Figs. 8 and 9), including cases where reflections arrive at times predicted from the independently derived velocity model (Fig. 2). Our observations of poor lower-crustal reflectivity beneath the FIR are consistent with wide-angle seismic observations from the FIRE program of a weak or nonexistent reflection from the Moho (P_mP phase) along the ridge (Smallwood et al., 1999) and with the lack of a clear Moho on receiver functions based on many teleseismic earthquakes recorded in western and eastern Iceland (Du et al., 2002).

Much remains to be learned about the seismic image response of fabrics created by igneous sill intrusion into the crust from the mantle or cumulate layering within cooling intrusive bodies. However, modeling studies based on observed igneous intrusions have thus far shown that actual cumulate layering is capable of producing a highly reflective seismic record (Deemer and Hurich, 1994). Singh and McKenzie (1993) and Singh et al. (1998) have developed forward models that demonstrate that lower-crustal reflectivity could result entirely from layering within an igneous body or from mantle-sourced magmatic underplating resulting from an interlayering of high- and low-velocity material. The expected magmatic underplating associated with the development of the overthickened FIR would therefore be anticipated to be capable of producing strong reflectivity in the lower crust (Farnetani et al., 1996; 2002; Fig. 12). Certainly, it is possible in a general sense to observe lower-crustal reflectivity from environments analogous to the FIR, as has been done over the Hawaiian volcanic island chain (Ten Brink and Brocher, 1987) and over the Réunion Hotspot (Charvis et al., 1999). Again, the fact that the FIR lower crust is poorly reflective indicates that not all magmatically underplated environments produce physical structures that can be seismically imaged. Our inference is somewhat analogous to the approach and observations of Bauer et al. (2003) from a deep seismic reflection profile over a mantle-derived Cretaceous composite mafic and alkaline igneous ring complex intruded in a continental rift setting in Namibia. Bauer et al. (2003) found that although the crust on either side of the intrusion displays layered lower-crustal reflectivity, the crust within the intrusion is seismically transparent throughout, although it shows both high reflection strength and weak reflection coherency, similar to our observations for the FIR. They explained their results

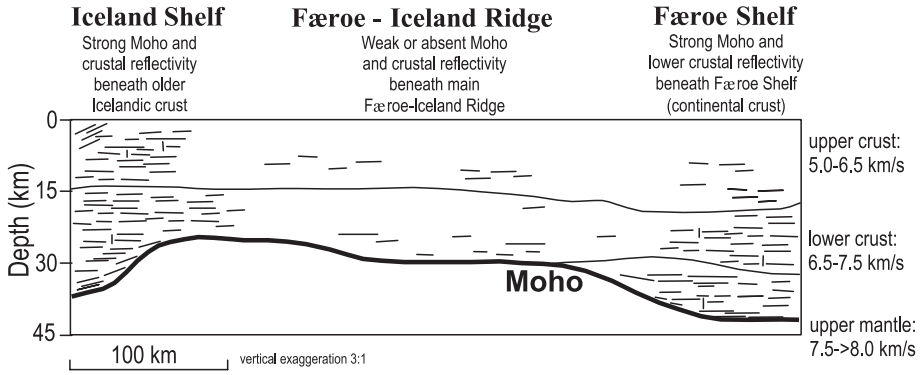

Fig. 12. Cartoon drawing of FIR crust and upper mantle indicating variation in reflectivity based on FIRE cmp reflection results (velocity and density information from Smallwood et al., 1999).

in terms of a network of subhorizontal and subvertical mafic intrusions within a ductile lower crust represented seismically as small-scale heterogeneities that cause weak reflection coherency due to destructive interference.

A vast literature exists on the seismic, geochemical, and petrologic origin and composition of the lower crust, even just for Iceland and the North Atlantic region (e.g., see Farnetani et al., 1996 and McKenzie and O'Nions, 1998). Here, we make a few suggestions on geologic processes that may have contributed to the lack or destruction of seismically imageable structure beneath the FIR. Competing models of oceanic crustal accretion have developed in response to the discovery of shallow lenses of melt beneath oceanic spreading centers versus observations of mafic sills at the base of exposed ophiolite bodies (see Maclennan et al., 2001a for a review). Models from the former observations suggest that melt is supplied directly from the mantle to a shallow magma chamber, which is then advected toward the base of the crust as the melt becomes solid (Henstock et al., 1993); however, the latter observations have also stimulated models in which crustal growth proceeds by the injection of small sills in the lower crust (Kelemen et al., 1997). Maclennan et al. (2001a) conclude that accretion beneath northern Iceland has taken place at both shallow and deep levels in the crust. The paucity of strong reflectivity along the FIR from the FIRE program could have therefore resulted from repeated dike injection, such that an early formed laminated crustal structure has been destroyed (Nelson, 1991; BABEL Working Group, 1991).

A more probable explanation for the inferred lack of strong physical property contrasts in the lower crust beneath the FIR is that the entire crust was hot at the time of formation. At present, the lower crust and uppermost mantle beneath Icelandic rift zones have been interpreted to have high temperatures and partially molten rock (Darbyshire et al., 2000a,b; Maclennan et al., 2001b). Barton and White (1997) have interpreted a mantle potential temperature for the FIR of 1550 °C based on seismic thickness and subsidence arguments, and Maclennan et al. (2001b) infer mantle temperatures of 1480–1520 °C above the present-day Icelandic mantle plume from geochemical arguments. If the lower crust and upper mantle were indeed relatively hot at the time of underplating or advection from shallower levels, then one might envisage a scenario where any sill-like bodies were subsumed into a hot mass or at least developed boundaries that were sufficiently diffuse so as to be incapable of producing a reflection.

In contrast, the intrusion of melts into colder, preexisting crust of continental type (Færoe Islands shelf) and of oceanic type (Icelandic shelf and mainland) did produce reflective lower crustal sections, presumably because the newly intruded igneous rock chilled against the colder preexisting rock. By shooting seismic profiles with unchanged acquisition and processing parameters along both the FIR and the continental and Icelandic shelves at either end of the FIR (except for a shorter streamer in one instance), we are able to conclude that these observed changes in lower-crustal reflectivity are caused by the changing geological conditions and not by any changes in acquisition or processing.

Acknowledgements

This work was funded by the UK Natural Environment Research Council, by the BIRPS Industrial Associates, by the Icelandic Science Foundation, and by the Division of Ocean Sciences of the U.S. National Science Foundation. The effectiveness of all phases of this project was greatly enhanced by the invaluable participation of Richard W. Hobbs. Data processing was performed by Western Geophysical under the direction of the BIRPS Core Group and also by using ProMAX2D™ under a Landmark University Grant. Reviews by two anonymous referees substantially improved the final version of the paper.

References

Allmendinger, R.W., Nelson, K.D., Potter, C.J., Barazangi, M., Brown, L.D., Oliver, J.E., 1987. Deep seismic reflection characteristics of the continental crust. Geology 15 (4), 304–310.

BABEL Working Group, 1991. Reflectivity of a Proterozoic shield: examples from BABEL seismic profiles across Fennoscandia. In: Meissner, R., Brown, L., Dürbaum, H.-J., Franke, W., Fuchs, K., Seifert, F. (Eds.), Continental Lithosphere: Deep Seismic Reflections, AGU Geodynamics Ser., vol. 22, pp. 77–86.

Barton, A.J., White, R.S., 1997. Crustal structure of Edoras Bank continental margin and mantle thermal anomalies beneath the North Atlantic. Journal of Geophysical Research B 2 (102), 3109–3130.

Bauer, K., Trumbull, R.B., Vietor, T., 2003. Geophysical images and a crustal model of intrusive structures beneath the Messum ring complex, Namibia. Earth and Planetary Science Letters 216, 65–80.

Bott, M.H.P., Gunnarsson, K., 1980. Crustal structure of the Iceland–Faeroe Ridge. Journal of Geophysical Research B 2 (47), 221–227.

Brown, L.D., 1987. Lower continental crust: variations mapped by COCORP deep seismic profiling. In: Blundell, D.J., Brown, L.D.Annales Geophysicae, vol. 5B, pp. 325–330.

Charvis, P., Laesanpura, A., Gallart, J., Hirn, A., Lépine, J.-C., de Voogd, B., Minshull, T., Hello, A., Pontiose, Y., 1999. Spatial distribution of hotspot material added to the lithosphere under La Réunion, from wide-angle seismic data. Journal of Geophysical Research B 2 vol. 104, 2875–2893.

Darbyshire, F.A., White, R.S., Priestley, K.F., 2000a. Structure of the crust and uppermost mantle of Iceland from a combined seismic and gravity study. Earth and Planetary Science Letters 181, 409–428.

Darbyshire, F.A., Priestley, K.F., White, R.S., Stefánsson, R., Gudmundsson, G.B., Jakobsdóttir, S.S., 2000b. Crustal structure of central and northern Iceland from analysis of teleseismic receiver functions. Geophysical Journal International 143, 163–184.

Deemer, S.J., Hurich, C.A., 1994. The reflectivity of magmatic underplating using the layered mafic intrusion analog. Tectonophysics 232, 239–255.

Du, Z., Foulger, G.R., Julian, B.R., Allen, R.M., Nolet, G., Morgan, W.J., Bergsson, B.H., Erlendsson, P., Jakobsdottir, S., Ragnarsson, S., Stefansson, R., Vogfjord, K., 2002. Crustal structure beneath western and eastern Iceland from surface waves and receiver functions. Geophysical Journal International 149, 349–363.

Farnetani, C.G., Richards, M.A., Ghiorso, M.S., 1996. Petrological models of magma evolution and deep crustal structure beneath hotspots and flood basalt provinces. Earth and Planetary Science Letters 143, 81–94.

Farnetani, C.G., Legras, B., Tackley, P.J., 2002. Mixing and deformations in mantle plumes. Earth and Planetary Science Letters 196, 1–15.

Henstock, T.J., Woods, A.W., White, R.S., 1993. The accretion of oceanic crust by episodic sill intrusion. Journal of Geophysical Research B 98, 4143–4161.

Hobbs, R.W., 2003. Seismic imaging of lower crustal heterogeneity. In: Goff, J.A., Holliger, K. (Eds.), Heterogeneity in the Crust and Upper Mantle Chapter 9. Kluwer Academic/Plenum Publishers, New York, pp. 237–255.

Hobbs, R.W., Peddy, C.P., 1987. Is lower crustal layering related to extension? In: Matthews, D., Smith, C. (Eds.), Deep Seismic Reflection Profiling of the Continental Lithosphere, Geophysical Journal of the Royal Astronomical Society, vol. 89, pp. 239–242.

Kelemen, P.B., Koga, K., Shimizu, N., 1997. Geochemistry of gabbro sills in the crust–mantle transition zone of the Oman Ophiolite: implications for the origin of the oceanic lower crust. Earth and Planetary Science Letters 146, 475–488.

Klemperer, S.L., 1988. Crustal thinning and nature of extension in the northern North Sea from deep seismic reflection profiling. Tectonics 7, 803–821.

Klemperer, S., Hobbs, R., 1991. The BIRPS Atlas Deep seismic reflection profiles around the British Isles. Cambridge University Press, New York.

Klemperer, S.L., White, N., 1989. Coaxial stretching or lithospheric simple shear in the North Sea? Evidence from deep seismic profiling and subsidence. In: Tankard, A.J., Balkwill, H.R. (Eds.), Extensional Tectonics and Stratigraphy of the North Atlantic Margins, AAPG Mem., vol. 46, pp. 511–522.

Klemperer, S.L., Hauge, T.A., Hauser, E.C., Oliver, J.E., Potter, C.J., 1986. The Moho in the Northern Basin and Range Province, Nevada, Along the COCORP 40 N Seismic Reflection Transect. Geological Society of America Bulletin 97, 603–618.

Levander, A., Hobbs, R.W., Smith, S.K., England, R.W., Snyder, D.B., Holliger, K., 1994. The crust as a heterogeneous "optical" medium, or "crocodiles in the mist". Tectonophysics 232, 281–297.

Maclennan, J., McKenzie, D., Gronvöld, K., Slater, L., 2001a. Crustal accretion under northern Iceland. Earth and Planetary Science Letters 191, 295–310.

Maclennan, J., McKenzie, D., Gronvöld, K., 2001b. Plume-driven upwelling under central Iceland. Earth and Planetary Science Letters 194, 67–82.

Matson, K.H., Paschal, D., Weglein, A.B., 1999. A comparison of three multiple-attenuation methods applied to a hard water-bottom data set. The Leading Edge 18 (1), 120–126.

McBride, J.H., England, R.W., 1999. Window into the Caledonian Orogen: structure of the crust beneath the East Shetland Platform, United Kingdom. Geological Society of America Bulletin 111, 1030–1041.

McKenzie, D., O'Nions, R.K., 1998. Melt production beneath oceanic islands. Physics of the Earth and Planetary Interiors 107, 143–182.

Meissner, R., Sadowiak, P., 1992. The terrane concept and its manifestation by deep reflection studies in the Variscides. Terra Nova 4, 598–607.

Meissner, R., Tanner, B., 1993. From collision to collapse: phases of lithospheric evolution as monitored by seismic records. Physics of the Earth and Planetary Interiors 79, 75–86.

Nelson, K.D., 1991. A unified view of craton evolution motivated by recent deep seismic reflection and refraction results. Geophysical Journal International 105, 25–35.

O'Connor, J.M., Stoffers, P., Wijbrans, J.R., Shannon, P.M., Morrissey, T., 2000. Evidence from episodic seamount volcanism for pulsing of the Iceland plume in the past 70 Myr. Nature 408, 954–958.

Prussen, E.I., 1991. The reflection Moho along the COCORP Northwest U.S. Transect. AGU Geodynamics Series 22, 315–322.

Reston, T.J., 1990. The lower crust and the extension of the continental lithosphere: kinematic analysis of BIRPS deep seismic data. Tectonics 9, 1235–1248.

Richardson, K.R., Smallwood, J.R., White, R.S., Snyder, D.B., Maguire, P.K.H., 1998. Crustal structure beneath the Faroe Islands and the Faroe–Iceland Ridge. Tectonophysics 300, 159–180.

Richardson, K.R., White, R.S., England, R.W., Fruehn, J., 1999. Crustal structure east of the Faroe Islands. Petroleum Geoscience 5, 161–172.

Saunders, A.D., Fitton, J.G., Kerr, A.C., Norry, M.J., Kent, R.W., 1997. The North Atlantic igneous province, in Large Igneous Provinces: Continental, Oceanic, and Planetary Flood Volcanism. American Geophysical Union Monograph 100, 45–93.

Singh, S.C., McKenzie, D., 1993. Layering in the lower crust. Geophysical Journal International 113, 622–628.

Singh, S.C., Hague, P.J., McCaughey, M., 1998. Study of the crystalline crust from a two-ship normal-incidence and wide-angle experiment. Tectonophysics 286, 79–91.

Smallwood, J.R., White, R.S., 2002. Ridge–plume interaction in the North Atlantic and its influence on continental breakup and seafloor spreading. In: Jolley, D.W., Bell, B.R. (Eds.), The North Atlantic Igneous Province: stratigraphy, Tectonic, Volcanic and Magmatic Processes, Special Publications-Geological Society of London, vol. 197, pp. 15–37.

Smallwood, J.R., White, R.S., Staples, R.K., 1998. Deep crustal reflectors under Reydarfjördur, eastern Iceland: crustal accretion above the Iceland mantle plume. Geophysical Journal International 134, 277–290.

Smallwood, J.R., Staples, R.K., Richardson, K.R., White, R.S., 1999. Crust generated above the Iceland mantle plume: from continental rift to oceanic spreading center. Journal of Geophysical Research 104, 22885–22902.

Staples, R.K., White, R.S., Brandsdóttir, B., Menke, W., Maguire, P.K.H., McBride, J.H., 1997. Faroe–Iceland Ridge Experiment: I. The crustal structure of north-eastern Iceland. Journal of Geophysical Research 102, 7849–7866.

ten Brink, U.S., Brocher, T.M., 1987. Multichannel seismic evidence for a subcrustal intrusive complex under Oahu and a model for Hawaiian volcanism. Journal of Geophysical Research, B 92, 13687–13707.

Warner, M.R., 1990. Basalts, water, or shear zones in the lower continental crust? In: Leven, J.H., Finlayson, D.M., Wright, C., Dooley, J., Kennett, C. (Eds.), Seismic probing of continents and their margins, Tectonophysics 173, pp. 163–174. 1–4.

Waagstein, R., 1988. Structure, composition and age of the Faeroe basalt plateau. In: Morton, A.C., Parson, L.M. (Eds.), Early Tertiary Volcanism and the Opening of the NE Atlantic, Special Publication-Geological Society of London, vol. 39, pp. 225–238.

Watts, A.B., Torne, M., Buhl, P., Mauffret, A., Pascal, G., Pinet, B., 1990. Evidence for reflectors in the lower continental crust before rifting in the Valencia trough. Nature 348, 631–635.

White, R.S., 1992. Crustal structure and magmatism of North Atlantic continental margins. Journal of the Geological Society (London) 149, 841–854.

White, R.S., 1997. Rift–plume interaction in the North Atlantic. Philosophical Transactions of the Royal Society of London. Series A 355, 319–339.

White, R.S., McKenzie, D., 1989. The generation of volcanic continental margins and flood basalts. Journal of Geophysical Research B 2 (94), 7685–7729.

White, R.S., McKenzie, D., 1995. Mantle plumes and flood basalts. Journal of Geophysical Research B 2 (100), 17543–17585.

White, R.S., Spence, G.D., Fowler, S.R., McKenzie, D.P., Westbrook, G.K., Bowen, A.N., 1987. Magmatism at rifted continental margins. Nature 330, 439–444.

White, R.S., McKenzie, D., O'Nions, R.K., 1992. Oceanic crustal thickness from seismic measurements and rare earth element inversions. Journal of Geophysical Research 97, 19683–19715.

White, R.S., McBride, J.H., Maguire, P.K.H., Brandsdóttir, B., Menke, W., Minshull, T.A., Richardson, K.R., Smallwood, J.R., Staples, R.K., 1996. Seismic images of crust beneath Iceland contribute to long-standing debate. Eos, Transactions, American Geophysical Union 77, 197–201.

Wiggins, J.W., 1988. Attenuation of complex water-bottom multiples by wave-equation-based prediction and subtraction. Geophysics 53, 1527–1539.

Yilmaz, O., 1987. Seismic data processing. Soc. Explor. Geophys., Tulsa. 526 pp.